ISSN 1062-8738, Bulletin of the Russian Academy of Sciences. Physics, 2014, Vol. 78, No. 10, pp. 988–995. © Allerton Press, Inc., 2014.
Original Russian Text © V.P. Pilyugin, T.P. Tolmachev, I.L. Solodova, O.V. Antonova, E.G. Chernyshev, A.I. Ancharov, A.M. Patselov, 2014, published in Izvestiya Rossiiskoi Akademii Nauk. Seriya Fizicheskaya, 2014, Vol. 78, No. 10, pp. 1238–1245.

Formation and Properties of Copper–Silver Solid Solutions upon Severe Deformation under Pressure

V. P. Pilyugin[a], T. P. Tolmachev[a], I. L. Solodova[a], O. V. Antonova[a], E. G. Chernyshev[a], A. I. Ancharov[b, c], and A. M. Patselov[a]

[a] *Institute of Metal Physics, Ural Branch, Russian Academy of Sciences, Yekaterinburg, 620990 Russia*
[b] *Institute of Solid-State Chemistry and Mineral Processing, Siberian Division, Russian Academy of Sciences, Novosibirsk, 630128 Russia*
[c] *Novosibirsk State University, Novosibirsk, 630090 Russia*
e-mail: pilyugin@imp.uran.ru

Abstract—Nonequilibrium nanocrystalline FCC solid solutions are obtained via the mechanical alloying of $Cu_{1.0-x}$–Ag_x powders (x = 0.1, 0.2, ..., 0.9, 1.0) with deformation under pressure and their properties are investigated. The chemical homogeneity, microstructure, mechanical properties, and thermal stability of the alloys are investigated. The alloys have the positive deviation of lattice parameters from the Vegard law with crystallite sizes of 20 nm, hardness exceeding the initial values of the components by 4.5–6 times, and a brittle character of fracture. The thermally induced decomposition of nonequilibrium solutions starts at temperatures close to room and is complete after heating to 500°C with the development of collective recrystallization.

DOI: 10.3103/S1062873814100189

INTRODUCTION

The Cu–Ag system has a positive mixing enthalpy of 5 kJ/mol [1] and a limited solubility of almost zero at $T \leq 293$ K [2], due to it violating the second Hume–Rothery rule. The system can be used to investigate mechanical alloying and the structure of alloys thanks to a number of its properties: (i) copper and silver are FCC isostructural elements; (ii) they have close melting points; (iii) they have comparatively low and close values of elastic moduli and binding energy; (iv) they have no intermetallic compounds under equilibrium conditions; and (v) diffusion and recovery upon and after strong deformation occur at ~293 K. The system is of interest as a material for dentistry and a metal restorer. The products of mechanical synthesis, usually obtained by ball milling, are in the powder state with the collection of disadvantages inherent to the milling method: contaminants, undesirable heating, and methodological limitations on investigation [3, 4]. For reliable structural attestation and measurements of the physical and mechanical properties of synthesized solutions [5], they must be prepared in the form of bulk and whole samples. High-pressure torsion (HPT) in a Bridgman chamber with puncheons made of superhard metal-ceramic materials WC-6 and c-NB is an acceptable method that allows us to synthesize and compact the materials in the form of whole samples [6]. This makes it possible to attain high degrees of deformation up to severe plastic deformation (SPD) [7] while controlling treatment parameters (pressure, temperature, and degree of deformation) without contaminating samples with material from the foreign bodies used to treat them.

EXPERIMENTAL

Mixtures of powders Ag (99.99%) and Cu (99.70%) (Fig. 1) of compositions $Cu_{1.0-x}$–Ag_x (x = 0.1, 0.2, ... 0.9, 1.0 were subjected to HPT at 293 K to degrees of $0.5 \leq \varepsilon \leq 8.1$ and more on the true logarithmic scale of deformations $\varepsilon = \ln\left(1 + \varphi^2 R^2 / h^2\right)^{1/2}$, where R is the radius from the anvils' axis of rotation, φ is the angle of revolution in radians, and h is the thickness of the disc samples. Silver was sawn from an ingot in the form of shavings 100–500 μm in size (Fig. 1a), while the copper powder after chemical reduction consisted of particles 30–100 μm is size (Fig. 1b). After HPT in the modes noted in [6], samples were prepared in a form of thin discs 100–120 μm thick and 5.0 or 10.0 mm in diameter. Force F of the samples' deformation resistance was measured in situ from angle of revolution $\varphi = 2\pi n$, where n is the number of revolutions. Shear stress τ for anvil radius R = 2.5 mm was calculated using the formula $\tau = \frac{3l}{2\pi R^3} F$, where l is the length of the arm transferring the force from the anvil to an ATsDS-1I-1 electron dynamometer while recording the signal using a computer. The mixtures were treated at angles $\varphi = 2\pi n$, n = 1.0, 3.0, 10.0, and 40.0, which corresponded to degrees of deformation ε = 4.1, 5.9, 7.1, and 8.1, respectively. This method allowed us to

obtain SPDs [7] but also results in nonuniformity of deformation over the radii of samples (anvil areas). To reduce such deformation nonuniformity, HPT treatment was performed gradually in a three-step mode [6], after which $n = 3 \times 10$. The samples were then uniformly colored with a tint that was determined by the concentration of components in the charge. In this case, hardness was independent of radius $H_{\mu(R=0)} \approx H_{\mu(R\neq 0)}$ of the samples. The structure was investigated by means of X-ray structural analysis (XRSA) with reflections from a sample's lateral surface in CuK_α radiation using a DRON-1 diffractometer, and with transmission synchrotron radiation (SR) $\lambda = 0.03685$ nm in a beam with a cross section of 0.3×0.3 mm^2 while recording on a MAR-345 detector [8]. Electron microscopy was performed with a JEM-200 CX transmission electron microscope (TEM), while the microfractography of lateral surfaces of diametral disc fractures was done using a QUANTA-200 scanning electron microscope (SEM). Two-dimensional diffraction patterns, obtained with synchrotron radiation via integration over all directions, were transformed in plots of dependence intensity–diffraction angle 2θ. Lattice constant a (nm) of alloys was calculated from the position of the peaks' center of gravity. Vickers microhardness H_μ was measured using a PMT-3 device under a load of 0.5 N. Hardness was measured and structural investigations were performed for fresh samples mechanically synthesized no more than 3–4 h beforehand. If the time between preparation and measurements was longer, the samples were stored at 77 K. To investigate the thermal stability of alloys, the samples were held at room temperature for two–three weeks or annealed stepwise at 300°, 400°, and 500°C for 5 min. To determine the effect of temperature on the alloying kinetics and form of fractures in the samples, our Cu_{80}–Ag_{20} mixture was deformed at both 293 K and the cryogenic temperature of 80 K [6]. Temperature was measured with a copper–constantan thermocouple. The samples were weighed using an electron balance accurate to 10^{-4} g.

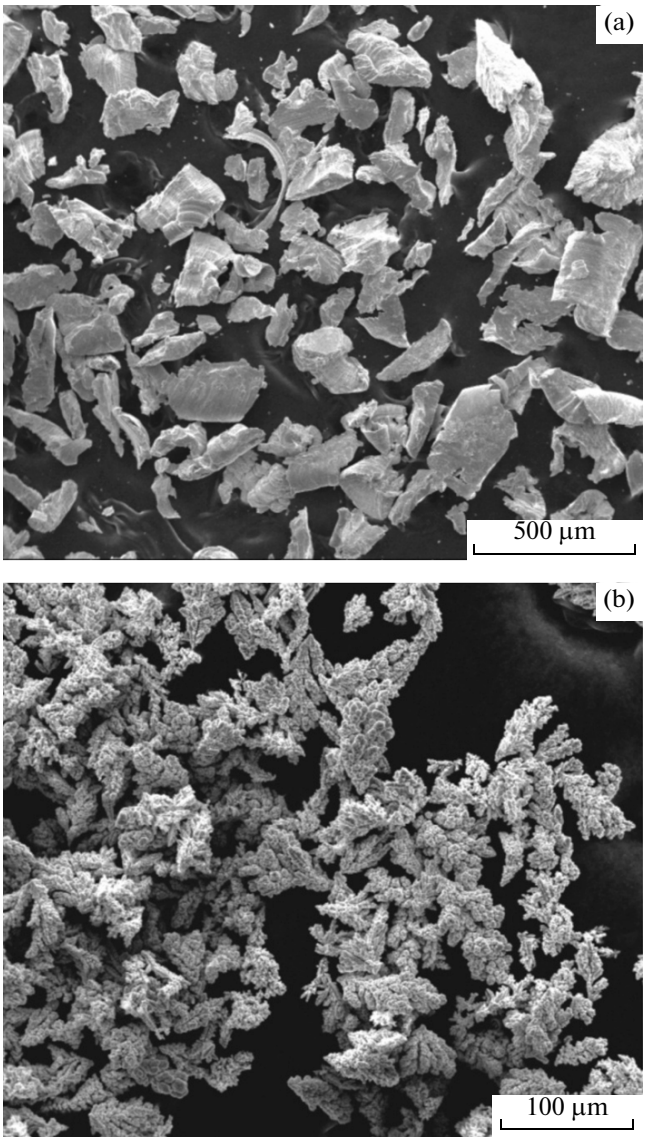

Fig. 1. Initial powders of (a) silver and (b) copper.

RESULTS AND DISCUSSION

The deformation of Cu and Ag powders and mixtures of them via axial compression of 8.0 GPa and combining compression with torsion allowed them to be compacted into whole disc samples.

Data from X-Ray Structural Analysis

Monotonically increasing deformation under pressure of pure components and their mixtures $Cu_{1.0-x}$–Ag_x (x = 0.1, 0.2, ... 0.9, 1.0)) produces structural-phase variations in them that are reflected in the relative intensity, shape, and location of lines of the Debye (Figs. 2a, 2b) and powder diffraction patterns (Fig. 3a). Mutually directed displacement of single-index peaks from copper and silver over angle scale 2θ is observed with growing deformation of the mixtures. Finally, displacement results in their merging completely into unique broad symmetric peaks for first-order reflections. For higher orders, the shape of reflections approach full symmetry but do not reach it (Fig. 3a). Based on the X-ray diffractometry data, we may conclude that our copper and silver were mechanically alloyed into an FCC structural substitutional solid solution upon cold (293 K) and very cold (80 K) SPD. Depending on the charge concentration of the mechanically synthesized alloys, the calculated unit cell parameters of the crystal lattice showed considerable positive deviation from Vegard's law (Fig. 4). The analytical dependence of lattice parameter $a(x_{Cu})$ con-

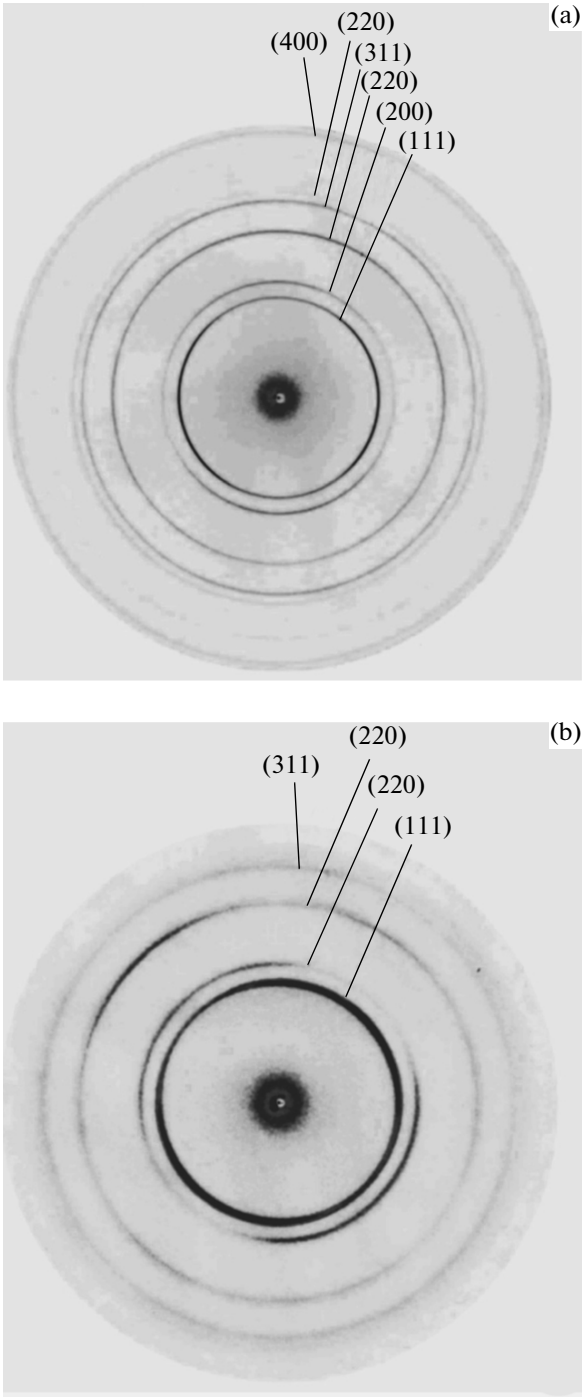

Fig. 2. Debye diffraction patterns in synchrotron radiation $\lambda = 0.03685$ nm of (a) deformed silver powder and (b) a Cu_{80}–Ag_{20} powder mixture.

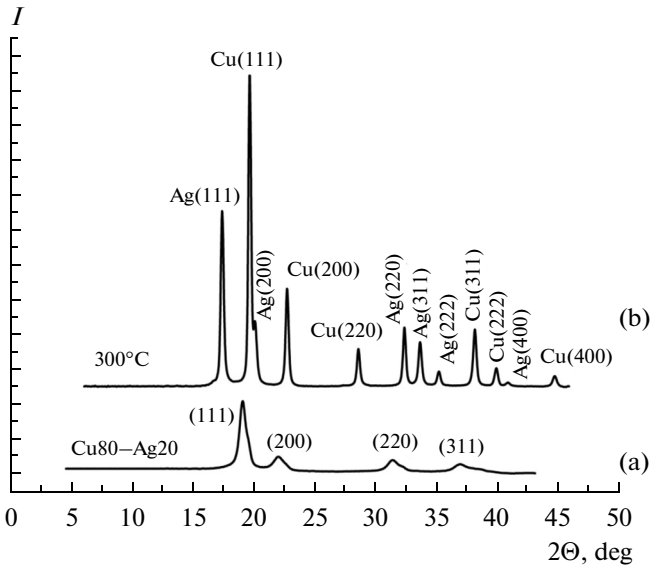

Fig. 3. X-ray diffraction patterns of samples with Cu_{80}–Ag_{20} composition (a) mechanically alloyed by three-step treatment at $T = 293$ K and (b) mechanically alloyed and annealed at 300°C for 5 min.

structed using the least-square method was expressed by a parabolic approximation:

$$a\ (\text{nm}) = 0.4037 - 2.544 \times 10^{-4} x_{Cu} - 4.644 \times 10^{-2} x_{Cu}^2,$$

where x_{Cu} is the atomic fraction of copper. Stepped annealing at 300, 400, and 500°C for 5 min caused the X-ray peaks of solid solutions to separate into the peaks of copper and silver and narrowed them, indicating the thermally induced decomposition of mechanically synthesized solid solutions and a reduction in internal stresses (Fig. 3b). Holding for 5 min at 500°C resulted in the complete decomposition of solid solutions, the onset of collective recrystallization, and the formation of copper oxide.

TEM Data

Electron microscopy investigations of the samples after SPD with $\varepsilon = 9.1$ ($n = 40$), or by the three-step mode with $n = 3 \times 10$, revealed the presence of microstructures with specific features. In the light-field image, the structure consists of separate light and dark fragments both irregularly shaped and with a shape approaching spherical in sizes of 10–25 nm. Segments of high-defect microstructure with agglomerations of separately unresolved high-density dislocations are observed. The average size of the round fragments in the Cu_{80}–Ag_{20} composition is d_{av} = 20–25 nm (Fig. 5a), with the maximum size reaching 50 nm. In addition to separate fragments, agglomerations of 5–20 light and dark spherical fragments are observed that differ in contrast from the surrounding regions. This is presumably explained by variations in the transmittance of the electron beam through the foil as a result of the different concentrations of copper and silver in the agglomerations. The intensity of the transmitted beam was reduced in segments richer in silver than the average initial charge and rose for silver-depleted segments, yielding microstructures in the form of dark and light agglomerations. According to the TEM and

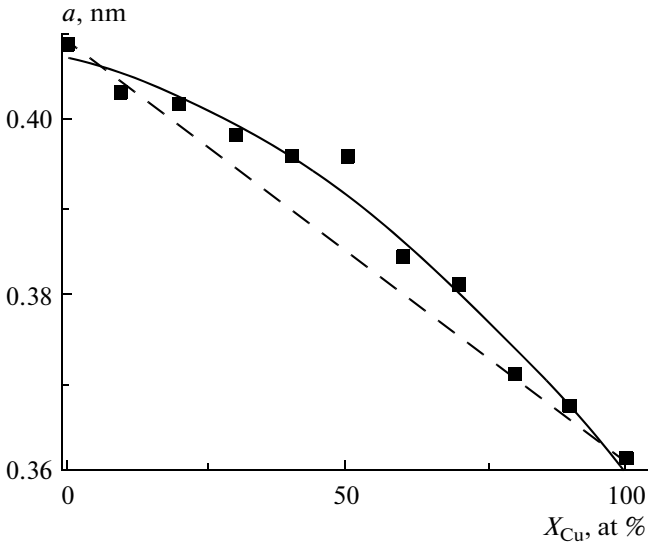

Fig. 4. Dependence of the lattice parameter (solid line) of mechanically synthesized Cu_{1-x}–Ag_x alloys (x = 0.1, 0.2, ..., 0.9, 1.0). The dashed line shows the linear dependence (Vegard's law).

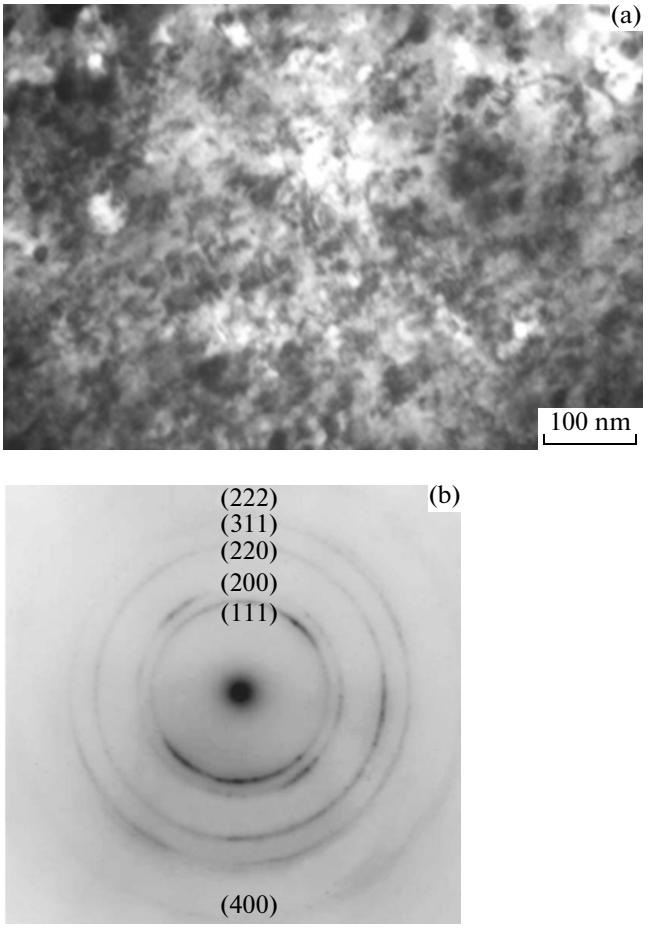

Fig. 5. Microstructure of a mechanically alloyed powder mixture of Cu_{80}–Ag_{20} composition after three-step treatment: (a) SEM light-field image and (b) electron microdiffraction. The low resolution is due to decomposition under the electron beam in the microscope's column.

XRSA data, the single-phase stage of FCC solid solution was obtained after SPD (Fig. 5b). Segments were observed in which Debye doublet rings were visible in the microdiffraction patterns, as with solutions of various concentrations. One more feature of the Cu–Ag microstructure observed in the electron microscope should be mentioned: Exposing the foil segments under the beam in the electron microscope column for 15–20 s or more led to variations in the form of fragments. The fragments become more rounded under the beam, and the contrast between light and dark agglomerations was enhanced. The behavior of the structure upon uncontrollable heating with the electron beam changed as a consequence of its unstable state, preventing us from obtaining a clear electron-microscopy image of the microstructure as it varied under the beam (Fig. 5). Storing the samples at 293 K for two weeks or more also produced a microstructure consisting of agglomerations of round fragments 20–50 nm in size with high contrast between white ones in a dark field and dark ones in a white field. The electron microdiffraction from such regions took the form of Debye doublet rings with superpositions of more intense point reflections from coarser crystallites.

Scanning Electron Microscopy of Fractures

The results from our investigation of the fractures in samples of Cu_{80}–Ag_{20}, HPT-treated with equal and growing deformations $\varepsilon = 4.8$ ($n = 1$), 5.9 (3), 7.1 (10), and 8.2 (40) at room (293 K) and cryogenic (80 K) temperatures, are presented in Fig. 6.

After compression of 8 GPa without revolution at room temperature, weakly elongated particles subjected to the initial deformation of extrusion from anvils were seen in fractures of samples. The particles were close to their initial shapes and gaps between the particles were observed in the center of samples, where extrusion deformation was minimal. Compression and revolution to deformation $\varepsilon = 4.1$ ($n = 1$) elongated the metal particles into parallel layers (Fig. 6a). There were gaps are between the layers that apparently appeared when the pressure dropped, cleaving the sample. At $\varepsilon = 5.9$ ($n = 3$), the samples thinned considerably (Fig. 6b). Gaps and cracks disappeared, segments with twisted layers were observed, and laminar elongation of the material combined with and was replaced by turbulent elongation. After high deformation $\varepsilon = 7.1$ ($n = 10$), a state was formed from the copper and silver powders whose fracturing could be characterized as brittle with the presence of short submicroscopic and microscopic necks. The residual thin lamination was anisotropic (Fig. 6c). The shape of fractures varied radically upon SPD with $\varepsilon = 8.1$ ($n = 40$) and three-step treatment. Preferentially

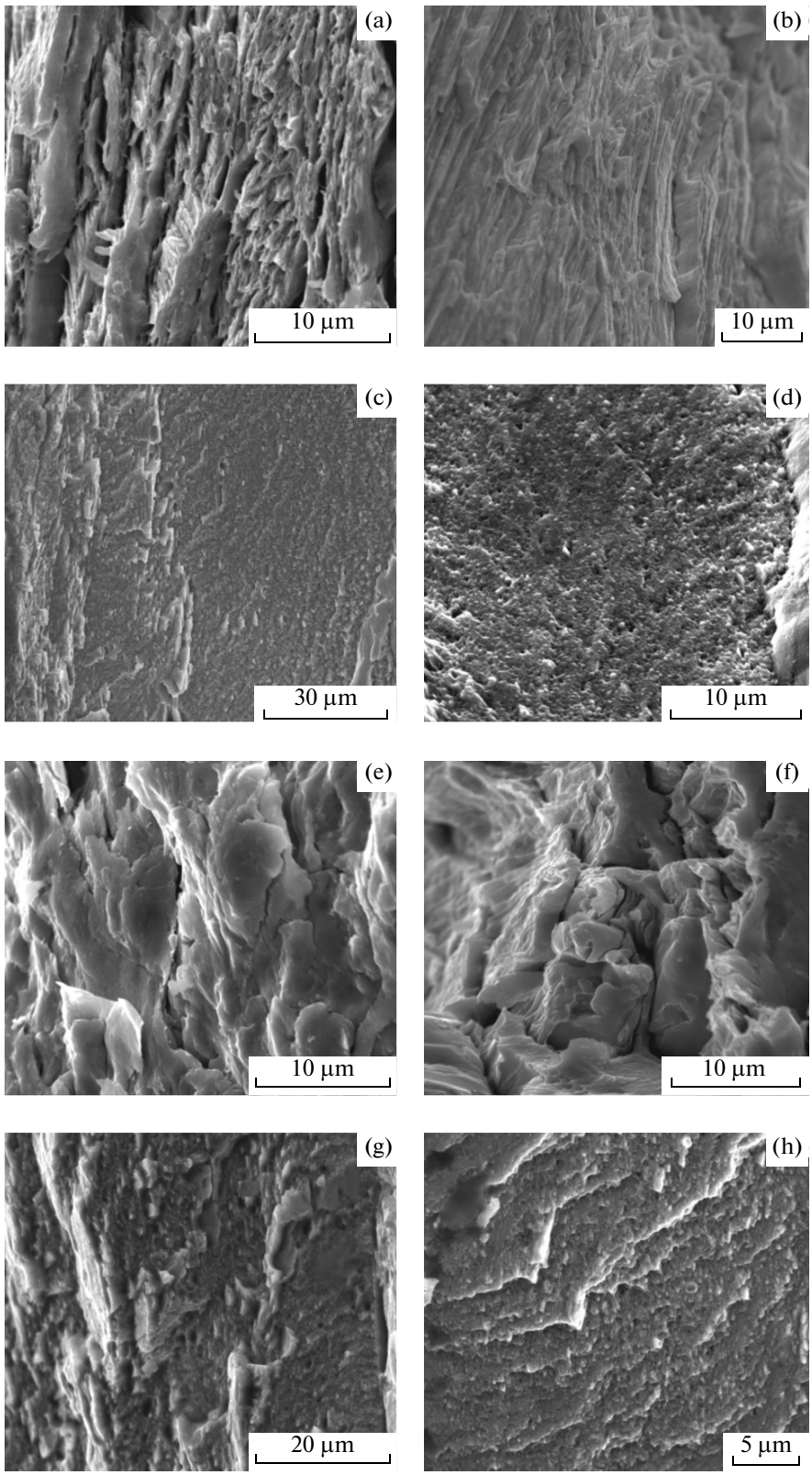

Fig. 6. Fractograms of samples of Cu_{80}–Ag_{20} composition after mechanical alloying at 293 K: (a) $a - \varepsilon = 4.1$ ($n = 1$), (b) 5.9 ($n = 3$), (c) 7.1 ($n = 10$), and (d) 8.1 ($n = 40$); and at 80 K: (e) $\varepsilon = 4.1$ ($n = 1$), (f) 5.9 ($n = 3$), (g) 7.1 ($n = 10$), and (h) = 8.1 ($n = 40$).

plane fractures of the sand type appeared with components of round and near-round shape on the submicron scale of 0.05–0.3 μm (Fig. 6d). If we return to the photo taken at $\varepsilon = 7.1$ ($n = 10$) (Fig. 6c), we can say (in light of the post-SP deformation (Fig. 6d) and allowing for scale) that the sand-like roughness of fractures began to form earlier, at $n = 10$, but in combination with residual microscopic exfoliations.

After the initial (in terms of cryogenic treatment) $\varepsilon = 4.1$ ($n = 1$) at 80 K, fractures in our Cu_{80}–Ag_{20} samples had the shape of flattened and elongated particles with gaps between them; lamination occurred but was less pronounced than after identical treatment at room temperature (Fig. 6e). Raising the treatment to $\varepsilon = 5.9$ ($n = 3$) led to considerable variation in the shape and mixing of metal particles, but segments of pure silver and copper still remained with gaps and cracks between them (Fig. 6f). The mixing, elongation of the particles, and twisting of the laminated formations occurred but were substantially delayed compared to the similar treatment at 293 K. Cryogenic deformation up to $\varepsilon = 7.1$ ($n = 10$) resulted in a nonuniform state at fractures: flat segments with the initial stages of a sand-like surface appeared, but there was still residual lamination (Fig. 6g). After low-temperature SPD with $\varepsilon = 8.1$ ($n = 40$), a more uniform state formed over the fractures, but the process was still not complete (Fig. 6h). Flat segments with sand-like roughness, sizes of 0.1–0.4 μm, and separate necks from residual lamination were observed (Fig. 6h). The drop in temperature required greater degrees of deformation to transition from one stage of deformation to another and to obtain the corresponding shape of fractures.

Shear Stress and Energy-Force Parameters of MP Deformation

Measurements of force F and calculated stresses τ of the resistance of samples to torsion on the degree of deformation for pure silver and copper powders showed their comparatively rapid attainment of saturation, notably at approximately $\varphi = \pi/2$ for silver and $\varphi = \pi$ for copper (Fig. 7). Reaching saturation τ for pure metals with no increase in strengthening $d\tau/d\varepsilon \to 0$ can be explained from the viewpoint of dynamic equilibrium being established between the competitive processes of strengthening and dynamic recovery. Mixtures of Cu–Ag powders showed higher resistance to deformation and reached saturation considerably later. This can be explained not only by the superposition of processes of structural fragmentation but also by the formation of solutions from Ag and Cu components and thus solid-solution strengthening (Fig. 7). The mechanical energy and force consumed by deformation was calculated from the measured resistance and the mass of samples. The specific energy per atom supplied to the Cu_{80}–Ag_{20} mixture at the stage close to saturation (i.e., refining the structure and forming

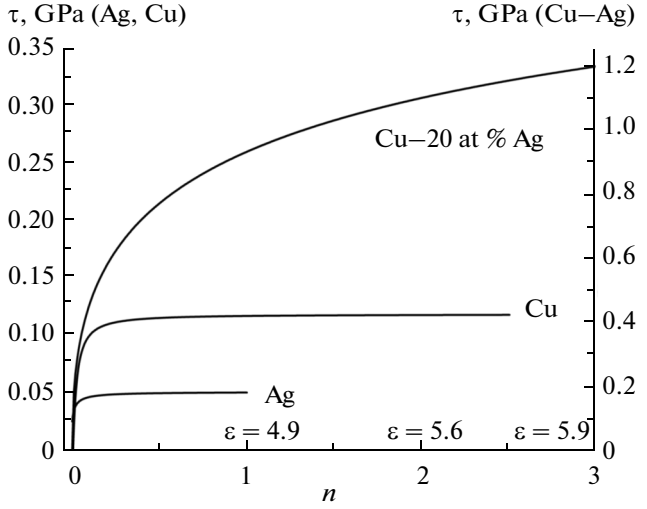

Fig. 7. In situ shear resistance during the torsion of silver, copper, and a mixture of Cu_{80}–Ag_{20} composition on the degree of deformation.

solutions) was 0.13 eV/atom per second, or 4.7% and 3.8% of the binding energy of the crystal lattices of silver and copper, respectively. This value is associated with the boundary between severe and extreme effect on the material [9]. HPT treatment with rotation rates two orders of magnitude higher is needed to move on to extreme processes for pumping energy into the system that is comparable to the energy of binding between atoms.

Microhardness and Plasticity

Measurements of the microhardness[1] in the middle of the radii of the SPD of disc samples for all $Cu_{1.0-x}$–Ag_x compositions ($x = 0.1, 0.2,, \ldots 0.9, 1.0$) allowed us to establish its dependence on the component content (Fig. 8). It should be noted that the values of H_μ for Cu–Ag alloys are high relative to the hardness of pure components and are comparable to the hardness of weakly quenched austenite steels (e.g., 12Kh18N10T stainless steel). Mechanically alloyed samples have greater brittleness than pure components, due to strong fragmentation and high levels of internal stress.

RESULTS AND DISCUSSION

The totality of the experimental data on the structure and properties of mechanically alloyed samples gives grounds for analyzing the processes and physical mechanisms behind the formation of Cu–Ag non-

[1] Note that in this case measuring microhardness is the same as measuring hardness, since the structural fragments number in the thousands and more are put into strongly fragmented structures by the indenter after MP deformation.

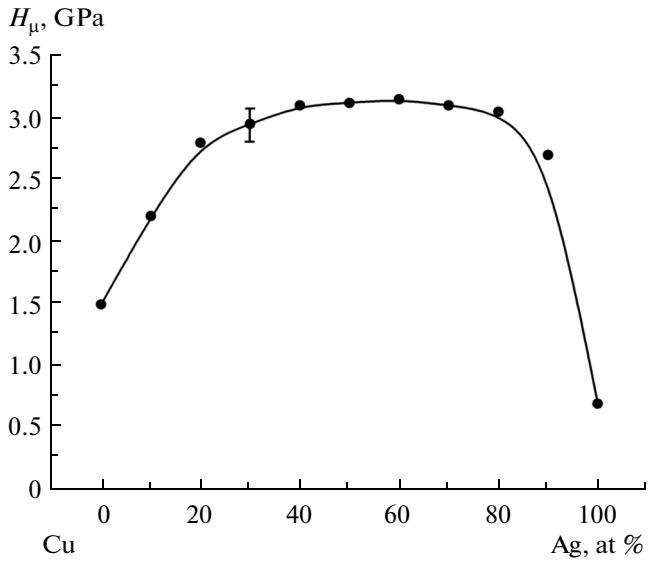

Fig. 8. Microhardness of $Cu_{1.0-x}$–Ag_x alloys (x = 0.1, 0.2, ..., 0.9, 1.0), obtained at room temperature.

equilibrium solid solutions and determining the their degree of homogeneity. The stage variations of single-phase pure metals during cold and very cold SPD were established in [11, 12]. Microstructures are subjected to saturation by defects of various topology and finally attain a nanostructured state that corresponds to anomalously high self-diffusion and the dynamic equilibrium mode $d\tau/d\varepsilon = 0$. This pattern is complicated considerably for mixtures of chemically heterogeneous metals and the heterogeneous mechanical diffusion associated with SPD. Deformation at meso- and microlevels leads to variation in the shape of metal particles, and the laminar elongation of particles with subsequent turbulent twists, turns, and breaks of layers begins. These processes strongly (by several orders of magnitude) expand the area of element contact. Interlayers of mixed states of elements are formed at contact interfaces of chemically heterogeneous metals. They are broadened and in turn subjected to structural variations up to the nanocrystalline state.

The complexity of the joint deformation of mixtures allows us to apply only qualitative models of mass transfer [5, 12–16] with flows of nonequilibrium point defects that are generated and vanish upon dragging of the thresholds of intersecting dislocations. Lowering the temperature to cryogenic (80 K) switches off the thermally activated mechanisms of the emergence and movement of dislocations. Mechanisms of double transverse sliding, climbing, or the dragging of thresholds are hampered or blocked. These phenomena notably reduce the formation and refinement of dislocation cellular structures and finally the nanofragmentation and mechanical formation of solid solutions [6, 11]. The calculated concentrations of equilibrium vacancies in copper and silver at 80 K are so low that they have no physical sense, and the observed cold (293 K) and especially very cold deformation (80 K) mass transfer must therefore be attributed entirely to the birth and annihilation of point defects of nonequilibrium concentration. In the dynamics of the SPD of Cu–Ag mixtures upon attaining dynamic equilibrium $d\tau/d\varepsilon = 0$, equilibrium formation of the solid solution and decomposition of the solid solution is established that corresponds to the conditions of pressure, temperature, and rate of deformation. The state is thus first of all at the limit of defect saturation, and the volume fraction of atoms in the intercrystallite space with d_{av} = 20 nm is as high as ~25–30% [10]. Second, the solid solution in the crystallite scale considerably exceeds the chemical equilibrium state with a mutual solubility of Cu and Ag of almost zero at 293 K [2]. Homological temperature $T_{hom} = T_{def}/T_m$, where T_{def} is the temperature of deformation and T_m is the melting point, is 0.07 and 0.24 for silver and 0.06 and 0.22 for copper at 80 and 293 K, respectively. Room temperature is too low to activate diffusion, although it is known that pure copper strongly deformed at 80 and 293 K undergoes dynamic and post-dynamic recrystallization [11], while collective recrystallization proceeds when it is stored and heated to 393 K.

In our case, the system is far from equilibrium immediately after deformation stops, both in terms of saturation with defects and with respect to the concentration of mixed copper and silver atoms; the system therefore shifts from dynamic equilibrium to decomposition of the solid solution immediately after SPD. Manipulations for removing shear stresses, hydrostatic stresses, preparing foils, and holding at 293 K thus cause the system to transition to a more stable state of initial decomposition. This was established by storing alloys at 293 K and heating them under the beam in a microscope column: the nonequilibrium solid solution decomposes, and globules of different contrast, enriched in copper or silver relative to the average charge composition, are formed. We therefore experimentally fixed the state of samples with regions retaining nonequilibrium solution and regions already subjected to decomposition. In addition, the microstructure of the resulting Cu–Ag alloys differed from those of the SPD of pure metals and alloys [10, 11] or mechanically alloyed solid solutions for systems with negative mixing enthalpies (e.g., Cu–Ni and Cu–Zn) [6]. In the latter, there were no globular crystallites after identical mechanical alloying since the decomposition processes were retarded. The fracturing of nonequilibrium Cu–Ag alloys can be qualitatively compared to the granular fracture in steels on the macrostructural scale, due to the chemical inhomogeneity of steel. A characteristic feature of granular fractures as a variety of stone-like fractures is the full coincidence of grain sizes in a structure and at a fracture [17].

CONCLUSIONS

Alloys with the structure of nanocrystalline FCC solid solutions were obtained during severe plastic deformation at 80 and 293 K for an Cu–Ag system with zero equilibrium solubility at room temperature and below. Solutions were chemically inhomogeneous on the scale of crystallites 20–25 nm in size and their agglomerations and had high degrees of hardness and brittleness. Cu–Ag alloys self-destruct according to an intercrystallite mechanism with the formation of sand-like surfaces at the submicroscopic level. The alloys are also unstable when held under the electron beam in a microscope column and are subject to decomposition upon heating. These features of non-equilibrium solid solutions of pure copper and silver powders should be considered when preparing and using them as solid lubricants, metal restorers, and materials for dentistry.

REFERENCES

1. Miedema, A.R., de Chatel, P.F., and de Boer, F.R., *Phys. B*, 1980, vol. 100, pp. 1–28.
2. Barabash, O.M. and Koval', Yu.N., *Kristallicheskaya struktura metallov i splavov* (Crystalline Structure of Metals and Alloys), Kiev: Naukova dumka, 1986.
3. Tian, Y.Z. and Zhang, Z.F., *Mater. Sci. Eng. A*, 2009, vol. 508, pp. 209–213.
4. Liu, J.B., Meng, L., and Zeng, Y.W., *Mater. Sci. Eng. A*, 2006, vols. 435–436, pp. 237–244.
5. Grigor'eva, T.F., Barinova, A.P., and Lyakhov, N.Z., *Mekhanokhimicheskii sintez v metallicheskikh sistemakh* (Mechanochemical Synthesis in Metallic Systems), Novosibirsk: Parallel', 2008.
6. Pilyugin, V.P., Tolmachev, T.P., Patselov, A.M., et al., *Deform. Razrush. Mater.*, 2013, no. 6, pp. 30–36.
7. Glezer, A.M., *Usp. Fiz. Nauk*, 2012, vol. 182, no. 5, pp. 559–566.
8. Ancharov, A.I., Manakov, A.Yu., Mezentsev, N.A., et al., *Nucl. Instrum. Methods A*, 2001, vol. 470, pp. 80–83.
9. Fortov, V.E., *Usp. Fiz. Nauk*, 2009, vol. 179, no. 6, pp. 653–687.
10. Andrievskii, R.A. and Glezer, A.M., *Fiz. Met. Metalloved.*, 2000, vol. 89, no. 1, pp. 91–112.
11. Voronova, L.M., Chashchukhina, T.I., Degtyarev, M.V., and Pilyugin, V.P., *Deform. Razrush. Mater.*, 2011, no. 3, pp. 9–11.
12. Pilyugin, V.P., Gapontseva, T.M., Chashchukhina, T.I., et al., *Fiz. Met. Metalloved.*, 2008, no. 4, pp. 1–11.
13. Gapontsev, V.L., Razumov, I.K., Gornostyrev, Yu.N., and Ermakov, A.E., *Fiz. Met. Metalloved.,* 2005, vol. 99, no. 4, pp. 26–37.
14. Farber, V.A., *Metalloved. Term. Obrab. Met.*, 2002, no. 8, pp. 3–9.
15. Skakov, Yu.A., *Metalloved. Term. Obrab. Met.*, 2004, no. 4, pp. 3–12.
16. Gapontsev, V.L., *Metalloved. Term. Obrab. Met.*, 2008, no. 5, pp. 48–55.
17. Bernstein, M.L., *Atlas defektov stali* (Atlas of Steels Defects), Moscow: Metallurgiya, 1979.

Translated by N. Korovin